Coupled thermo-electromechanical effects in quantum dots and nanowires

Patil, S. R., Melnik, R.V.N., Tsviliuk, O.

Proc. SPIE, Quantum Dots and Nanostructures: Synthesis, Characterization, and Modeling VII, Eds. Eyink, K. G., Szmulowicz, F., Huffaker, D. L., Vol. 7610, pp. 76100X-76100X-9 (2010), San Francisco, USA, 2010.

Coupled Thermo-electromechanical Effects in Quantum Dots and Nanowires

S. R. Patil[1], R.V. N. Melnik[1,*], O.I. Tsviliuk[2]
[1] M[2]NeT Laboratory,Wilfrid Laurier University, 75 University AvenueWest, Waterloo, ON, N2L 3C5, Canada
[2] JSC "RB", 1-3 Pivnychno-Syretska St, Kyiv 04136, Ukraine,

ABSTRACT

We report some results on the analysis of thermo-electromechanical effects in low dimensional semiconductor nanostructures (LDSNs). A coupled model of thermoelectroelasticity has been applied to the analysis of quantum dots and quantum wires. Finite element solutions have been obtained for different thermal loadings and their effects on the electromechanical properties in quantum dots and quantum wires are presented. Our model accounts for a practically important range of internal and external thermoelectromechanical loadings. Results are obtained for typical quantum dot and quantum wire systems with cylindrical geometry. The comparative analysis of thermoelectromechanical effects in quantum dots and quantum wires is also presented. It is observed that the electromechanical effects in LDSNs are noticeably influenced by thermal loadings. The influence is more significant in quantum dots as compared to that of quantum wires.

Keywords: thermo-electromechanical effects, quantum dots, quantum wires, coupled models of thermoelectroelasticity, low dimensional nanostructures

INTRODUCTION

Spatial confinement of electron motions in low dimensional semiconductor nanostructures (LDSNs) is attracting increasing attention of physics and engineering communities due to their current and potential applications. LDSNs are strained structures as they are normally embedded in a host material with different structural properties [1]. Advances in growth technologies now make it possible to grow high quality nanostructures. As these nanostructures are often formed through heteroepitaxy, they exhibit lattice mismatched strain, strain-induced piezoelectric, spontaneous polarization, coupled thermoelectromechanical and nonlinear electromechanical effects [2-4]. Apart from this, nanoscale size effects also lead to piezoelectricity in non-piezoelectric materials. Several studies show that the electromechanical effects play a key role in engineering electronic and optoelectronic properties of quantum dots (QD) and quantum wires (QWs) along with other LDSNs [1-4]. In particular, these effects are important in the transitions of type-I to type-II semiconductor heterostructures, rigid shifts in band edges and modifications of valance band structures [1], as well as in asymmetric wavefunctions in crescent QWs. Strain and piezoelectric effects are being used as tuning parameters in band gap engineering [4]. Electromechanical effects are therefore important in semiconductor nanostructures as most of the semiconductors are piezoelectric in nature.

*rmelnik@wlu.ca; Tel.: +1-519-884-1970 (ext. 3662) Fax: +1-519-884-9738, www.m2netlab.wlu.ca

Quantum Dots and Nanostructures: Synthesis, Characterization, and Modeling VII, edited by Kurt G. Eyink, Frank Szmulowicz, Diana L. Huffaker, Proc. of SPIE Vol. 7610, 76100X · © 2010 SPIE · CCC code: 0277-786X/10/$18 · doi: 10.1117/12.841310

On the other hand, thermal effects coupled with electric and mechanical fields in LDSNs have also become important. Indeed, as thermoelectric and thermoelastic effects are often significant in LDSNs, it is reasonable to expect that the temperature may also be used as a tuning parameter in band gap engineering [4]. One of the difficulties related to this lies with the fact that the novel LDSN-based electronic and optoelectronic devices may face challenges for thermal management. It is expected that by integrating LDSN materials into critical regions of microelectronic circuits,

the excess heat that limits device performance will be effectively removed. In addition, there are also many practical situations where interaction of thermopiezoelectric bodies with other media such as acoustic and fluid needs to be accounted for and the present formulation can act as a foundation for study of the resulting coupled models in the context of nanostructures. The study of fully coupled thermoelectromechanical effects in QWs has both technological as well as fundamental interest.

Therefore, a systematic study on thermal loadings is required for analyzing and optimizing their effects in LDSNs. In this paper, we apply a mathematical model describing coupled thermoelectromechanical effects in LDSNs, its special cases and generalizations [4]. Our particular focus is on the influence of thermoelectromechanical effects on properties of QDs and QWs in particualr for GaN/AlN QD and QW systems, as representatives of III–V group semiconductors. These semiconductors are wurtzite (WZ) crystals and are also known as potentially important thermoelectric materials. In our study we take a sufficiently wide range of thermal loadings of our structures, from 300K to 700K, keeping in mind their potential applications as thermoelectrics and their operations in various temperature regimes. The comparative analysis of thermoelectromechanical effects in quantum dots and quantum wires is also presented.

THEORETICAL FORMULATION

We formulate a mathematical model in order to study thermoelectromechanical effects in QDs and QWs. A general two-dimensional (2D) axisymmetric model is developed with coupled multi-physics governing equations. The model is based on a coupled system of equilibrium equations of elasticity, electrostatics and heat transfer. The linear fundamental equations for the thermoelectromechanical body occupying volume Ω, under steady state conditions, in our case can be summarized as follows:

$$\nabla \bullet \sigma = F, \qquad \nabla \bullet D = q. \tag{1}$$

Here σ is stress tensor and D is electric displacement vector, F and q are mechanical body force and electric charge in Ω, respectively. Note that, at the thermal equilibrium, the temperature change becomes spatially independent and the problem is governed by the equations (1) only.

We consider cylindrical QDs and QWs which are axisymmetric around z-axis (geometric details of which are given in Fig. 1). Governing equations for wurtzite (WZ) structures are axisymmetric, hence the solution of the model is axisymmetric as well. The material constants for the crystal with WZ symmetry used in this work are given in [4]. The original three-dimensional problem can be reduced in to a simpler two-dimensional problem by assuming axisymmetry along z-axis. The electromechanical balance equations in this case take the following form [5]:

$$\frac{\partial \sigma_{rr}}{\partial r} + \frac{\partial \sigma_{rz}}{\partial z} + \frac{\sigma_{rr} - \sigma_{\theta\theta}}{r} = 0, \quad \frac{\partial \sigma_{rz}}{\partial r} + \frac{\partial \sigma_{zz}}{\partial z} + \frac{\sigma_{rz}}{r} = 0, \quad \frac{\partial D_r}{\partial r} + \frac{\partial D_z}{\partial z} + \frac{D_r}{r} = 0 \tag{2}$$

These equations are invariant with respect to rotations around the *z*-axis, hence solutions can be separated into a (*r, z*) part and a θ part, subject to adequate boundary conditions. The constitutive relations then take the following form for WZ nanostructures:

$$\begin{aligned}
&\sigma_{rr} = C_{11}\varepsilon_{rr} + C_{12}\varepsilon_{\theta\theta} + C_{11}\varepsilon_{zz} - e_{31}E_z - \beta_1\Theta, \quad \sigma_{rz} = C_{44}\varepsilon_{rz} - e_{15}E_r, \\
&\sigma_{zz} = C_{13}\varepsilon_{rr} + C_{13}\varepsilon_{\theta\theta} + C_{33}\varepsilon_{zz} - e_{33}E_z - \beta_3\Theta, \quad D_r = e_{15}\varepsilon_{rz} - \in_{11} E_r \\
&D_z = e_{31}\varepsilon_{rr} + e_{31}\varepsilon_{\theta\theta} + e_{33}\varepsilon_{zz} - \in_{33} E_z + p_3\Theta + P_z^{SP}.
\end{aligned} \tag{3}$$

Note that based on the total differential of the general thermodynamic potential with Taylor series expansion of differentials of electromechanical quantities a generalization of Eq. (3) to the nonlinear case can be derived [4]. To take into account the lattice mismatch, the strain tensor components take the following form:

$$\varepsilon_{rr} = \frac{\partial u_r}{\partial r} - \varepsilon_a, \quad \varepsilon_{zz} = \frac{\partial u_z}{\partial z} - \varepsilon_c \quad \varepsilon_{rr} = \frac{u_r}{r} - \varepsilon_a, \quad \varepsilon_{rz} = \frac{1}{2}\left(\frac{\partial u_z}{\partial r} + \frac{\partial u_r}{\partial z}\right) \tag{4}$$

with $\varepsilon_a=(a_m-a_Q)/a_Q$ and $\varepsilon_c=(c_m-c_Q)/c_Q$ inside the QD and QW. Quantities a_m, c_m and a_Q, c_Q are the lattice constants of the matrix and the QD/QW, respectively, while quantities ε_a and ε_c are the local intrinsic strains (lattice mismatch) along the *a* and *c* directions, respectively. The directions *a* and *c* correspond to the shorter and longer dimensions of the unit cell of the wurtzite crystal, respectively.
The hydrostatic strain component is given by

$$\varepsilon_{vol} = \varepsilon_{rr} + \varepsilon_{zz} + \varepsilon_{\theta\theta}$$

The hydrostatic strain component is particularly important due to the fact that it provides information about rigid shift in energy subbands. In the plane stress case, by applying a 2D analytical method, it can be defined as in [1]:

$$\varepsilon_{vol} = 2\varepsilon_a\left(\frac{1-2\nu}{1-\nu}\right)$$

The misfit strain in the case of the GaN/AlN system is -2.47% and -4.07% in *a* and *c* directions, respectively. We assume that the QDs and QWs are oriented such that the *c*-direction of the crystal is along the *z*-axis. As the substrate is relatively large compared to the QD, we follow common practice to neglect lattice mismatch inside the matrix. The electromechanical parameters used in the calculations are given in [4]. All our numerical experiments have been performed under the condition for the relative errors between successive refinements to be less than 10^{-7}. In our case it has been achieved with around 10^6 triangular elements. Numerical solutions reflect the effect of the decreasing computational error when the solution approaches the boundary of the domain. Our results in figures 2–5 clearly depict this feature.

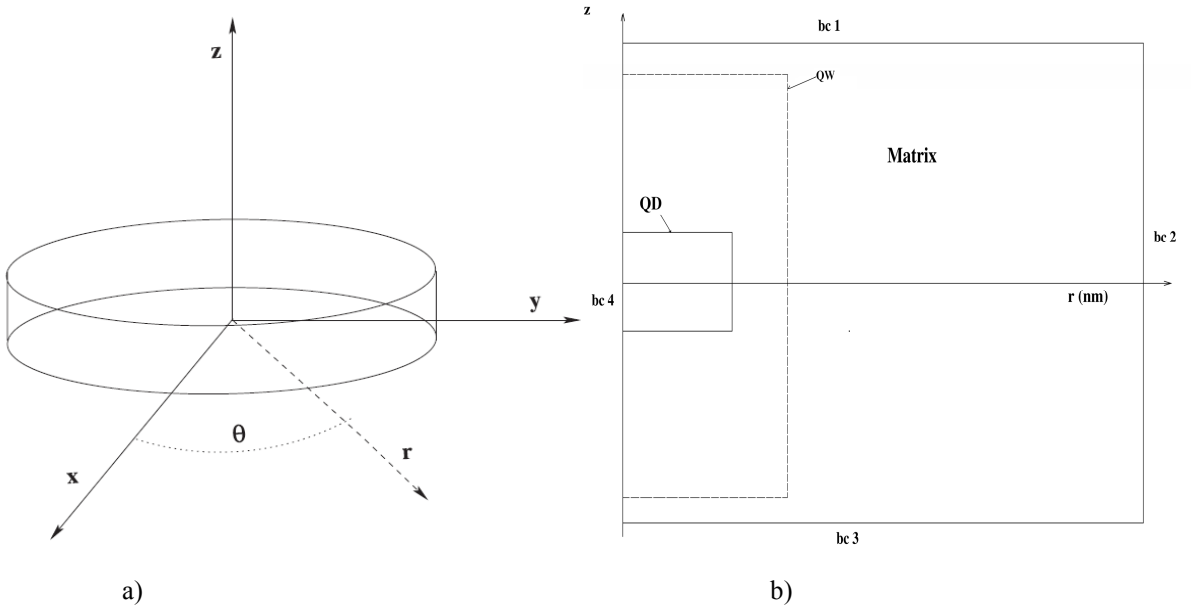

Figure 1. Geometry and co-ordinate system for the QD and QW systems in the (r, z) plane. (a) Co-ordinate system, (b) cylindrical QD and QW system.

RESULTS AND DISCUSSION

We discuss here our results for WZ GaN/AlN QD systems, as a representative example, geometric details of which are given in Fig. 1. Dirichlet boundary conditions are imposed along boundaries 1, 2, and 3 (see figure 1), while

$$u_r = 0 \text{ and } \quad \frac{\partial u_z}{\partial r} = \frac{\partial V}{\partial r} = 0$$

at boundary 4 (denoted by bc4 in figure 1). Due to the axisymmetry of the system (equations, geometry and boundary conditions) there is no angular dependence. The QD is of radius 5nm and of height 10 nm while the QW is 2 micron long and has radius of 100 nm.

Figure 2 shows the electromechanical distributions in QD at 300K. Fig. 2 a) and 2 b) show distributions of ε_{rr} and ε_{zz} in r-z plane, respectively. The magnitude of both the strain components, ε_{rr} and ε_{zz}, is observed to be less than about 1% and 2%, respectively, at all points inside the QD, except for the region near the edges where the strain has higher magnitude. ε_{rr} has its highest magnitude at the centre of the QD however ε_{zz} has it at the edge in r-direction. The QD causes the surrounding matrix to become strained and the strain decays slowly to zero away from the QWR. Thus strain relaxation occurs over most of the QD area. The electric potential (Fig. 2c) develops across the top and bottom of the QD, i.e. along the z-direction and has a magnitude of ~2.9V. As a result of this, electric field is seen to have highest magnitude at the centre of the QD. The highest magnitude of electric field is ~6×10^8 V/m. Our results agree well with previous reports [4].

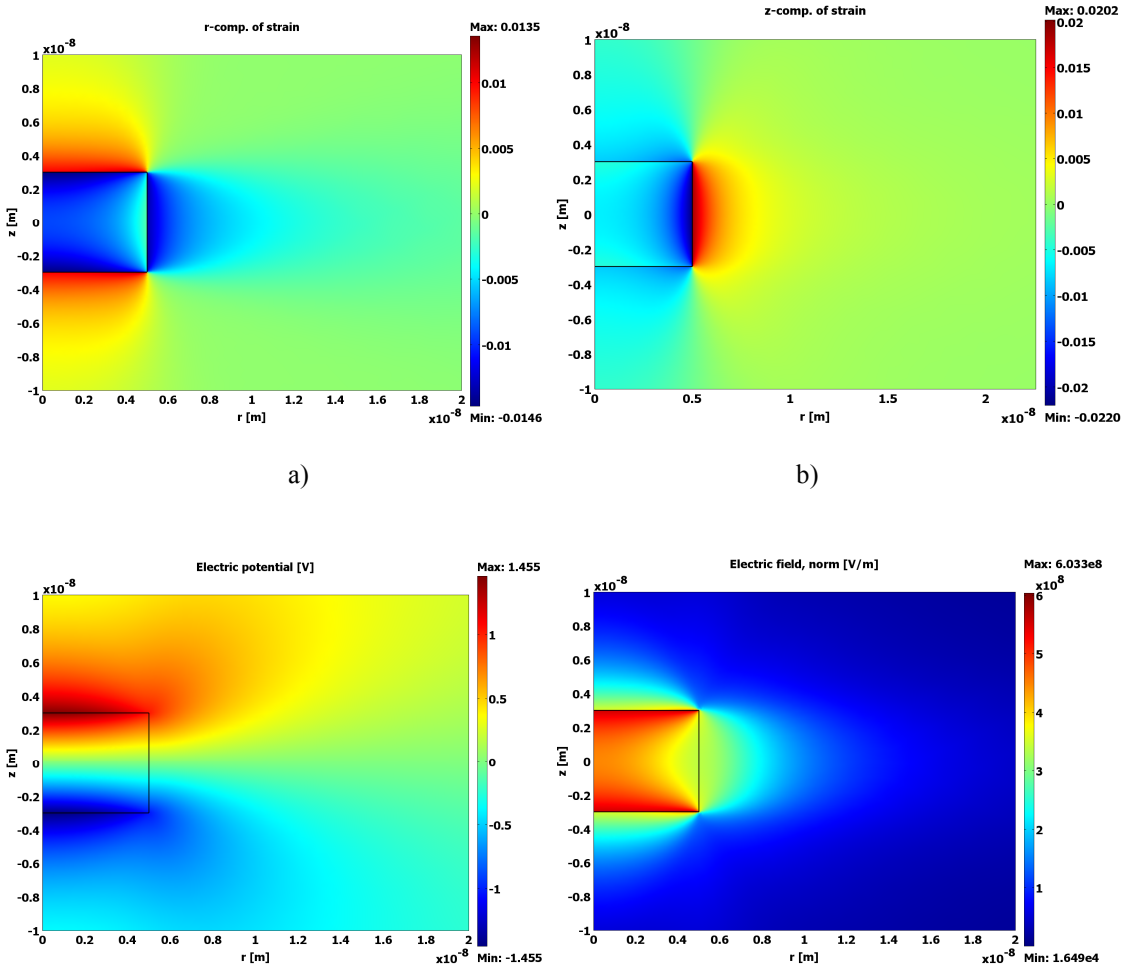

Figure 2 shows the electromechanical distributions in QD at 300K. a) r-component of strain b) z-component of strain, c) electric potential d) electric field.

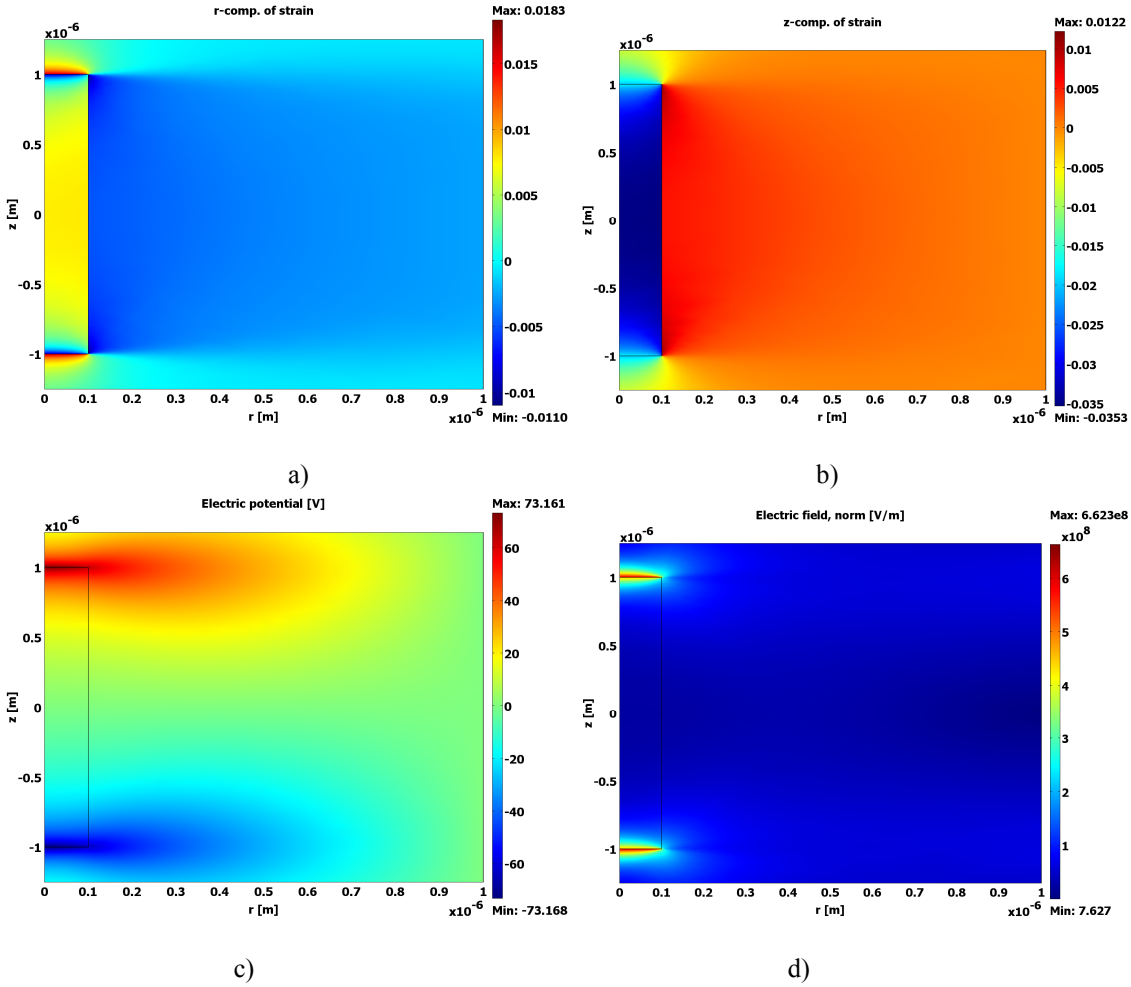

Figure 3 shows the electromechanical distributions in QW at 300K. a) r-component of strain b) z-component of strain, c) electric potential d) electric field.

Figure 3 shows the electromechanical distributions in the QW at 300K. Fig. 3 a) and 3 b) show distributions of ε_{rr} and ε_{zz} in the *r*-*z* plane, respectively. In contrast to the QD ε_{rr} has its lowest magnitude at the centre of the QW and ε_{zz} has it at the centre. Due to a relatively large structure, significant strain relaxation occurs over most of the wire area. However, the electric potential (Fig. 2c) develops across the top and bottom of the QD, i.e. along the z-direction. As a result of this, the electric field is seen to have its lowest magnitude at the centre of the QD and has its higher maginudes near the top and bottom edges. The highest magnitude of electric field is slightly higher than that of QD, i.e. ~6.6 x10^8 V/m.

Figure 4 shows the effect of temperature on electromechanical quantities for the cylindrical GaN/AlN QDs. Inside the QD, the magnitude of ε_{rr} (along the *z*-axis at $r = 0$, figure 4(a)) decreases with an increase in temperature. At the center of the QD the magnitudes are ~0.8% at 300 K and ~0.6% at 700 K. The magnitude of ε_{rr} decreases towards zero (unstrained region) faster at higher temperature than at lower temperature. As seen from figure 4(b), ε_{zz} is negative everywhere for all temperatures. The magnitude of ε_{zz} at the centre of the QD, i.e. at $z = 0$, is ~0.67% at 300 K, which increases with an increase in temperature to ~0.85% at 700 K. The potential difference across the top and bottom of

the QD decreases with an increase in temperature, from 2.9 V at 300 K to 2.8 V at 700 K (figure 4(c)). The electric field E exceeds 5.5MV/cm near the edges of the QD (figure 4(d)). Inside the QD, the E decreases with an increase in temperature, for example, at the center of the QD, $E = 4.5$ MVcm^{-1} at 300 K and $E = 4.8$ MVcm^{-1}at 700 K. Our results at 300 K are in excellent agreement with recent theoretical and experimental reports [4].

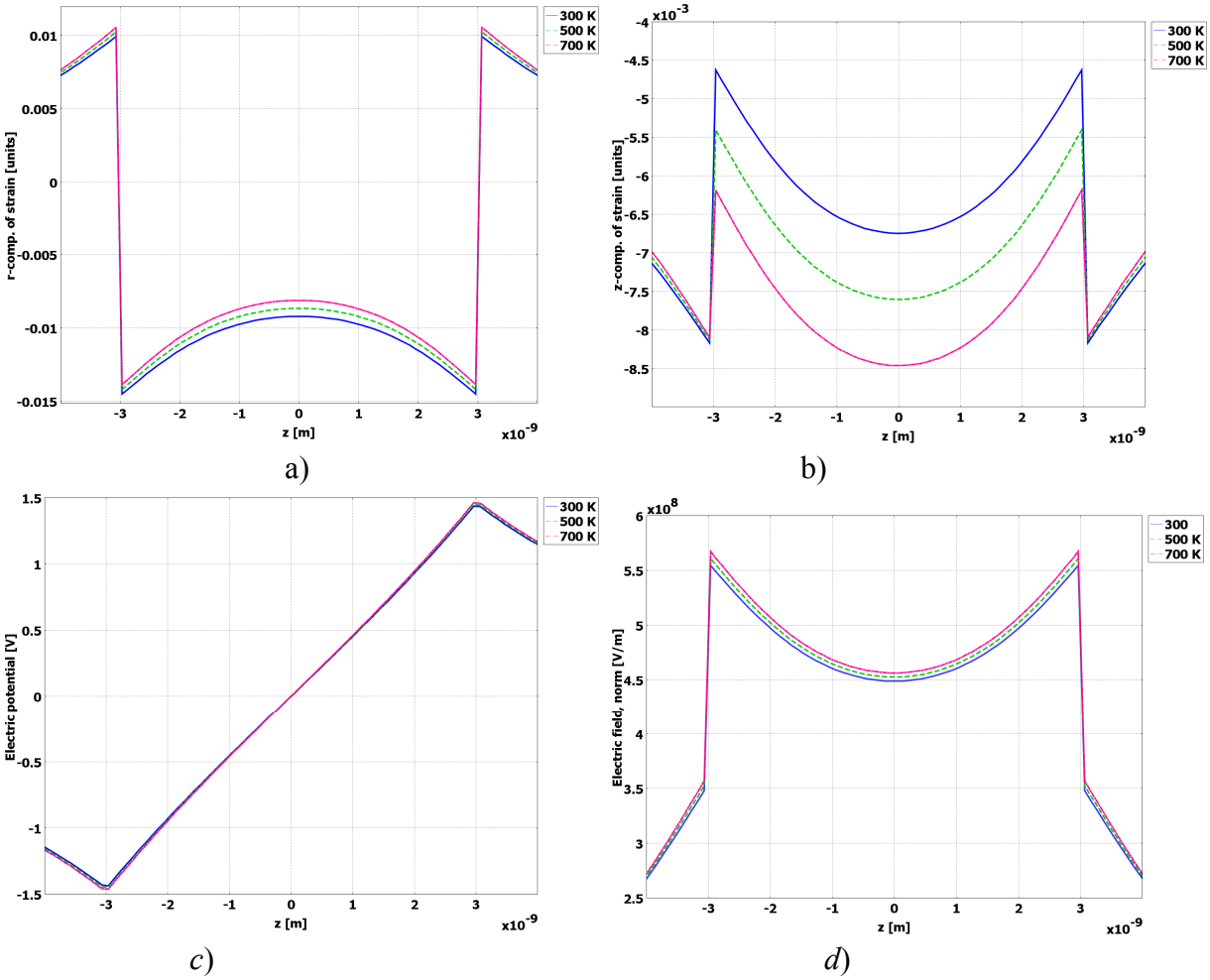

Figure 4. Effect of temperature on electromechanical quantities for cylindrical GaN/AlN QDs, (a) Strain, ε_{rr} , (b) strain, ε_{zz} , (c) electric potential, V, (d) electric field, E .

Figure 5 shows the effect of temperature on electromechanical quantities for the cylindrical GaN/AlN QWs. Inside the QW, the magnitude of ε_{rr} (along the z-axis at $r = 0$, figure 5(a)) decreases with an increase in temperature. In contrast to the QDs the r-component of strain has positive values in QWs, at the centre of the QW: at 300K, ε_{rr}=0.7% and at 700K ε_{rr}=0.8. The magnitude of ε_{zz} at the centre of the QW, i.e. at $z = 0$, is ~0.35% at 300 K, which decreases with an increase in temperature to ~0.34% at 700 K. The potential difference across the top and bottom of the QW decreases with an increase in temperature (figure 5(c)). The electric field E exceeds 5MV/cm near the edges of the QW (figure 5(d)). Inside the QD, the E is almost constant with respect to temperature, at the centre of the QD, E = 0.25 MV/cm at 300 K.

From table 1, it can be seen that electromechancial parameters are less sensitive in the case of QWs as compared to QDs. This is due to the large area available for electromechanical relaxation. Hence, we conclude that the QW system is more stable with respect to thermopiezoelectric effects compared to the QD. An order of magnitude smaller electric field is observed in QWs as compared to QD, signifies that the QWs will require less amount of carrier concentration in order to generate optical gain. The smaller magnitudes of electric potential and electric field represent an advantage of CdTe
based nanostructures over GaN as the latter structures face a problem of higher carrier density for generating optical gain [6].

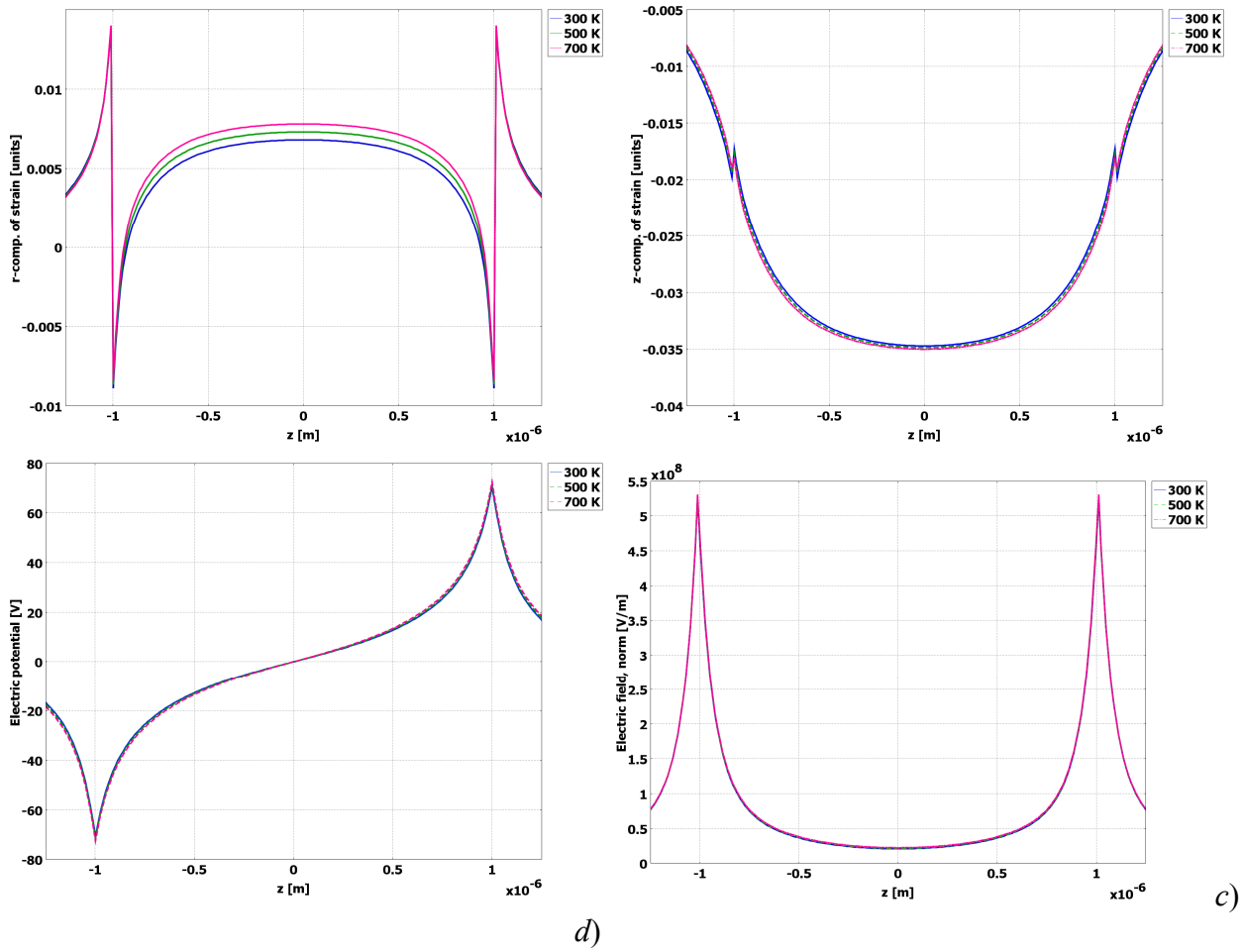

Figure 5. Effect of temperature on electromechanical quantities for cylindrical GaN/AlN QWs, (a) Strain, ε_{rr} , (b) strain, ε_{zz} , (c) electric potential, V, (d) electric field, E .

Table 1. Electromechanical parameters values in QD and QW at 300K at *r=z=0.*

	QD		QWR	
	300K	700K	300K	700K
r-comp. of strain [%]	0.8	0.6	0.7	0.8
z-comp. of strain [%]	0.67	0.85	0.35	0.34
Electric field [x10^8V/m]	4.5	4.7	0.25	0.25

SUMMARY

The influence of thermal loadings on electromechancial properties of LDSNs has been analyzed using a fully coupled thermoelectroelasticity model. It has been observed that the electromechanical properties vary noticeably with temperature. However, QDs are relatively more sensitive to the temperature as compared to the QWs. An order of magnitude smaller electric field has been observed in QWs as compared to QDs, signifies that the QWs will require less amount of carrier concentration in order to generate optical gain. The results indicate that QWs have advantages over their QD counterparts, in particular with respect to the carrier density in generating optical gain. Thermally less sensitive electromechanical properties of CdTe/ZnTe LDSNs may lead to thermally more stable performance which is important in preserving superior optoelectronic properties of nanostructures.

REFERENCES

1. Patil S.R. and Melnik R.V.N., "Coupled electromechanical effects in II–VI group finite length semiconductor nanowires," J. Phys. D: Appl. Phys. 42, 145113 (2009)
2. Liu W. and Balandin A. A. , "Thermoelectric effects in wurtzite GaN and $Al_xGa_{1-x}N$ alloys," J. Appl. Phys. 97, 123705 (2005)
3. Patil S.R. and Melnik R.V.N., "Thermopiezoelectric effects on optoelectronic properties of CdTe/ZnTe quantum wires", physica status solidi (a), 206, 960-964 (2009)
4. Patil S.R. and Melnik R.V.N., "Thermoelectromechanical effects in quantum dots," Nanotechnology, 12, 125402 (2009)
5. Melnik, R.V.N., "Generalised solutions, discrete models and energy estimates for a 2D problem of coupled field theory", Applied Mathematics and Computation, 107(1), 27-55 (2000).
6. Bernardini F. Fiorentini V. and Vanderbilt D., "Spontaneous polarization and piezoelectric constants of III-nitrides", Phys. Rev. B 56, R10024 (1997).